Publication No. U-1625

RESEARCH LABORATORIES

TECHNICAL REPORT

STUDY OF DETONATION BEHAVIOR OF SOLID PROPELLANTS

FIRST QUARTERLY REPORT

Prepared for:	Department of the Navy Bureau of Weapons Washington 25, D. C.
Under Contract:	NOw 62-0503-c, Task 1
Prepared by:	M. H. Boyer D. \. Schermerhorn

20 April 1962

AERONUTRONIC
A DIVISION OF Ford Motor Company
FORD ROAD / NEWPORT BEACH, CALIFORNIA

62-3-1

AERONUTRONIC

ABSTRACT

The present status of the one-dimensional computer routine is discussed including recent modifications in the grain burning phase of the reaction process. Calculations of minimum pressure for initiation of TNT are presented and compared with experimental values. Use of such comparisons for determining the rate parameters of the ignition process are considered.

Calculations are also presented on the detonation behavior of a typical composite double-base propellant. Minimum pressures for initiation, reaction and pressure profiles through the wave, and wave trajectory, are shown. The material is found to be marginal for support of a steady state detonation.

The theoretical backgound for the planned experiments on the equation of state of solids is discussed.

CONTENTS

ILLUSTRATIONS

SECTION 1

INTRODUCTION

This report presents the most recent developments in the one-dimensional treatment of detonation. In particular, the procedures for handling the energy distribution between solid and gaseous phases now appear to be satisfactory. Provision has been made for two grain burning processes which may conform either to a surface ignition regressive grain burning model, or to a point ignition progressive grain burning model. It is next planned to incorporate these provisions into the two-dimensional computer routine, and when this is accomplished, it is believed that the procedures for pressure-initiated detonation will be essentially complete. During the remainder of the program it is planned to undertake calculations designed to investigate the conformity between computed and experimental behavior. An important part of this latter step is the work on experimental study of the equation of state of propellant and explosive materials which is presently in progress.

Work on thermal initiation of detonation has been held in abeyance pending the development of operational procedures capable of providing acceptable computer running times.

SECTION 2

MATHEMATICAL DEVELOPMENTS

Two modifications were made to the one-dimensional computer routine during this report period. The first of these is concerned with the computation of energy distribution between solid and gaseous phases in the detonation waves; the second is concerned with adaptation to a point ignition internal grain burning model which, as discussed in the last progress report, appears to be more pertinent to the detonation of homogeneous materials than the external surface burning model presently used.

The problem of energy distribution between phases was discussed to some extent in the last quarterly report. The specific methods used to solve this problem were found to be unsatisfactory because the solution became unstable a short time after ignition of the charge. This instability was subjected to considerable study during the reporting period, and was found to be caused by a coupling of small oscillations in the values of v_s, e_s and p. In order to avoid this behavior, it now appears necessary to compute v_s, v_g by the integration of equations defining the relation between dv_s, dv_g and $d\bar{v}$. These are derived as follows.

Considering first the dv_g, the term is assumed to depend upon the sum of two effects, the first to be derivable from the compression or expansion of a mixture of solid and gas, with simultaneous transfer of material from the solid to the gas phase, the second to be derivable from the addition of heat to the gas phase, at constant average volume. (Some changes have been made in the nomenclature used in this program. New definitions are given at the end of the report.)

First, one has:

$$de_s = - pdv_s \tag{1}$$

From the solid equation of state:

$$(p + \beta)v_s = (\gamma_s - 1) e_s + C \tag{2}$$

$$(p + \beta)dv_s + v_s\, dp = (\gamma_s - 1)\, de_s = - (\gamma_s - 1)\, pdv_s$$

Then:

$$(\frac{\beta}{p} + \gamma_s)\, pdv_s = - v_s\, dp$$

$$\frac{d\ln p}{d\ln v_s} = - (\frac{\beta}{p} + \gamma_s) \tag{3}$$

And for the gas ($\beta = 0$)

$$\frac{d\ln p}{d\ln v_g} = - \gamma_g \tag{4}$$

Also:

$$(1 - f_s)\, v_g + f_s v_s = \bar{v}$$

$$(1 - f_s)\, dv_g - v_g df_s + f_s dv_s + v_s df_s = d\bar{v} \tag{5}$$

From (3) and (4)

$$\frac{dv_g}{dv_s} = \frac{v_g}{v_s}\, \frac{(\gamma_s + \beta/p)}{\gamma_g}$$

Combining with (5) and solving for dv_g;

$$dv_g' = \frac{d\bar{v} - (v_s - v_g)\, df_s}{1 - f_s\left[1 - \frac{v_s \gamma_g}{v_g(\gamma_s + \beta/p)}\right]} \tag{6}$$

The effect of heat addition to the gas phase at constant average volume has been discussed in previous reports.[1] Considering the following diagram for one gram of material:

gas phase	solid phase
$\bar{vol} = v_g f_g$	$vol = v_s f_s$

$$f_g de_g = dE - f_g p dv_g \tag{7}$$

$$f_s de_s = p f_s dv_s \tag{8}$$

From the equation of state:

$$de_s = \frac{1}{\gamma_s - 1}\left[(p + \beta)\, dv_s + v_s\, dp\right] \tag{9}$$

$$de_g = \frac{1}{\gamma_g - 1}\left[p dv_g + v_g dp\right] \tag{10}$$

Also:

$$dv_s = -\frac{1 - f_s}{f_s} dv_g \tag{11}$$

Elimination of dp, de_s, de_g and dv_s between equations 7-11 gives

$$dv_g'' = \frac{(\gamma_g - 1)\quad dE}{(1 - f_s)\, p\, \gamma_g + (p\gamma_s + \beta)\frac{v_g}{v_s}\,\frac{(1 - f_s)^2}{f_s}} \tag{12}$$

One then has

$$dv_g = dv_g' + dv_g''$$

By similar methods, the expression for dv_s is found to be:

$$dv_s = \frac{d\bar{v} - (v_s - v_g)\, df_s}{f_s + (1 - f_s)\frac{v_g}{v_s}\,\frac{(\gamma_s + \beta/p)}{\gamma_g}} \qquad (13)$$

and

$$de_s = -p dv_s$$

In order to treat materials with a self-reactive binder, an additional grain burning equation has been added to the scheme, identical in form with the one presently used but having different rate parameters and associated with a different heat of reaction. This requires an additional term in the calculation of the chemical heat release. The previous differential equations are then differenced to give the following computational procedure:

IGNITION PHASE

Treated as before

GRAIN BURNING PHASE

Set initial conditions:

$$e_s^o = \bar{e}^o$$

$$f_2^o = 1 \; ; \quad f_2^1 = 1\text{-}F_1$$

$$f_3^o = 1 \; ; \quad f_3^1 = 1\text{-}F_1 \qquad (14)$$

$$f_4^o = 1\text{-}F_1$$

$$(f_2^{n+1})^{1/3} = (f_2^n)^{1/3} - \frac{B_2 \Delta t^n p^m}{p^{m/w+1}} \exp\left[\frac{-A_2}{e_s^n + Q_2' / \gamma_g^n}\right] \qquad (15)$$

$$(f_3^{n+1})^{1/3} = (f_3^n)^{1/3} - \frac{B_3 \Delta t^n p^m}{p^{m/w+1}} \exp\left[\frac{-A_3}{e_s^n + Q_3' / \gamma_g^n}\right] \quad (16)$$

$$f_4^{n+1} = 0.8 \exp(-D^{n+1}) + 0.2 \exp(-4D^{n+1}) \quad (17)$$

$$D^{n+1} = (D_s + \frac{Do}{p^n}) \pi^2 (t^{n+1} - \tau) \quad (18)$$

$$f_s^{n+1} = F_2 f_2^{n+1} + F_3 f_3^{n+1} + F_1 \quad (19)$$

$$v_s^{n+1} = v_s^n + \frac{(\bar{v}^{n+1} - \bar{v}^n) - (v_g^n - v_s^n)(f_s^n - f_s^{n+1})}{f_s^{n+1} + (1 - f_s^{n+1})\left(\frac{v_g}{v_s}\right)^n \left(\frac{\gamma_s^n + \beta/p^n}{\gamma_g}\right)} \quad (20)$$

$$v_g^{n+1} = v_g^n + \frac{(\bar{v}^{n+1} - \bar{v}^n) - (v_g^n - v_s^n)(f_s^n - f_s^{n+1})}{1 - f_s\left[1 - \frac{v_s^n}{v_g^n}\frac{\gamma_g^n}{\gamma_s^n + \beta/p^n}\right]} \quad (21)$$

$$+ \frac{(\gamma_g^n - 1)\left[(e_s^n - e_g^n)(f_s^n - f_s^{n+1}) + F_2 Q_2 (f_2^n - f_2^{n+1}) + F_3 Q_3 (f_3^n - f_3^{n+1}) + Q_4 (f_4^n - f_4^{n+1})\right]}{(1 - f_s^{n+1})\left[p^n \gamma_g^n + (p^n \gamma_g^n + \beta)\left(\frac{v_g}{v_s}\right)^n \left(\frac{1 - f_s^{n+1}}{f_s^{n+1}}\right)\right]}$$

$$\gamma_s^{n+1} = \gamma_{go} + \left[\frac{b}{v_s^{n+1}} + \left(\frac{b}{v_s^{n+1}}\right)^2\right](\gamma_{go} - 1) \quad (22)$$

$$\gamma_g^{n+1} = \gamma_{go} + \left[\frac{b}{v_g^{n+1}} + \left(\frac{b}{v_g^{n+1}}\right)^2\right](\gamma_{go} - 1) \quad (23)$$

$$p^{n+1} = (\gamma_g^{n+1} - 1)\left[e^{-n} - \frac{f_s^{n+1}}{\gamma_s^{n+1} - 1}(\beta v_s^{n+1} - C) + F_2Q_2(f_2^n - f_2^{n+1}) + F_3Q_3(f_3^n - f_3^{n+1})\right.$$

$$\left. + Q_4(f_4^n - f_4^{n+1}) - (p^n + 2q^{n+1/2})\left(\frac{\bar{v}^{n+1} - \bar{v}^n}{2}\right)\right] / \left[\bar{v}^{n+1}\right.$$

$$\left. + \left(\frac{\gamma_g^{n+1} - \gamma_s^{n+1}}{\gamma_s^{n+1} - 1}\right) f_s^{n+1} v_s^{n+1} + (\gamma_g^{n+1} - 1)\left(\frac{\bar{v}^{n+1} - \bar{v}^n}{2}\right)\right] \qquad (24)$$

$$\bar{e}^{n+1} = \bar{e}^n - (p^n + p^{n+1} + 2q^{n+1/2})\left(\frac{\bar{v}^{n+1} - \bar{v}^n}{2}\right) + F_2Q_2(f_2^n - f_2^{n+1})$$

$$+ F_3Q_3(f_3^n - f_3^{n+1}) + Q_4(f_4^n - f_4^{n+1}) \qquad (25)$$

$$e_s^{n+1} = e_s^n + (p^n + p^{n+1} + 2q^{n+1/2})\left(\frac{v_s^{n+1} - v_s^n}{2}\right) \qquad (26)$$

$$e_g = \frac{p^{n+1} v_g^{n+1}}{\gamma_g^{n+1} - 1} \qquad (27)$$

Other details of the program remain the same.

The second modification concerning adaptation of the routine to an internal grain burning model has turned out to be relatively straightforward. It was shown in the previous progress report[2] that the grain burning rate laws for the two models are identical if f is defined in the external burning case as the fraction of material unburned, and in the internal burning case as the fraction of material burned. It follows very readily that conversion from the former to the latter problem can be accomplished by changing the sign of Q_2, Q_3, B_2 and B_3 in the input, and redefining the initial values of the f's as follows:

$$f_2^o = 0 \qquad f_2^1 = F_1$$
$$f_3^o = 0 \qquad f_3^1 = F_1 \qquad (28)$$

Integration is terminated when $f \geq 1$.

The proper procedure for f_4 is somewhat in doubt with this model. However, the diffusion rate law is significant here only in the case of composite double-base propellants with grain size of the order of 5 microns or less. If it can be assumed that the centers of ignition are located in the interface between oxidizer grain and binder, then the most reasonable procedure is to use the same geometry for the diffusion process in both models. Although this may falsify to some extent the form of the diffusion reaction profile through a detonation wave, it would not significantly affect the reaction zone length and so should not appreciably alter detonation behavior.

SECTION 3

CALCULATIONS

The one-dimensional program in the form described in Section 2 has been used to examine the detonation behavior of TNT and of a representative composite double-base propellant. Input data for the two materials is as shown in Table I except as noted in the illustrations. The external-regressive grain burning formulation of the grain burning reaction was used in these cases.

Of particular importance in calculating the detonation behavior of real materials is the selection of proper values for the rate parameters A_1, A_2, B_1 and B_2. Data for TNT are available from two sources. The first of these consists of thermal decomposition studies; this source has been reviewed and used by Cook.[3,4] The second consists of experimental work carried out at the Naval Ordnance Laboratory on the shock pressures necessary for initiation of detonation in TNT.[5] Such pressures are strongly dependent upon the values used for B_1 and A_1 and the data can therefore be used to evaluate these parameters if the other needed information about the material is available. As has been discussed in previous reports, the assumption that the ignition zone is a high-temperature region in the vicinity of a bubble or void which has been passed over by a shock, leads to the postulate

$$A_1 = A_2/2$$

$$B_1 = B_2$$

TABLE I

INPUT DATA FOR CALCULATION

TNT	Common	Composite Double Base
$C = 795$ cal/gm	$a = 4.0 \times 10^{-8}$	$C = 664$ cal/gm
$\beta = 50$ kbar	$\gamma_o = 1.3$	$\beta = 50$ kbar
$Q_1 = 1130$ cal/gm	$b = 1.03$	$Q_1 = 622$ cal/gm
$Q_2' = Q_2 = 1130$ cal/gm	$D_s = 10^{-4}$ cm^2/sec	$Q_2' = Q_2 = 380$ cal/gm
$Q_3' = Q_3 = 0$	$D_o = 10^{-1}$ cm^2/sec	$Q_3' = Q_3 = 864$ cal/gm
$Q_4 = 0$	$w = 20$ kbar	$Q_4 = 0$
$A_1/R = 4715^\circ$K	$m = 1$	$A_1/R = 5500^\circ$K
$A_2/R = 9430^\circ$K		$A_2/R = 11{,}000^\circ$K
$B_1 = 1.08 \times 10^{13}$		$A_3/R = 19{,}400^\circ$K
$B_2 = 1.08 \times 10^{13}$		$B_1 = 1.6 \times 10^{12}$
$B_3 = 0$		$B_2 = 1.6 \times 10^{12}$
$F_1 = 0.01$		$B_3 = 4.6 \times 10^{15}$
$F_2 = 0.99$		$F_1 = 0.01$
$F_3 = 0$		$F_2 = 0.205$
$F_i = 0$		$F_3 = 0.470$
$Z = 0.14$ cm		$F_i = 0.315$
$P_a = 1.5$ gm/cm^3		$Z_2 = 2.5 \times 10^{-3}$ cm
$P = 93.8$ kbar		$Z_3 = 12 \times 10^{-3}$ cm
$t_p = 1.5\ \mu$sec		$\rho_a = 1.80$ gm/cm^2
		$P = 100$ kbar
		$t_p = 4\ \mu$sec

The procedure for obtaining values of the rate parameters is to compare computed values of the minimum pressure for initiation of detonation obtained with different values of A_1 and B_1 with the experimental value. The computed values are obtained by setting B_2 and B_3 equal to zero so that the grain burning reactions are suppressed, and by using a low value of F_1 so that the ignition reaction alone is not capable of supporting a detonation wave. The calculation is initiated by an imposed shock of $\sim$100 kbars having a duration of 1.5 μ sec, which is heavy enough to cause ignition. This disturbance then propagates into the material as a fading wave, and the maximum wave pressure at the last zone which ignites is the minimum pressure for initiation.

Figure 1 shows the trajectory of such a fading wave obtained with values of A_1 and B_1 derived from the data of Cook. This gives directly

$$A_2 = 43{,}400 \text{ cal/mol}$$

$$B_2 = 1.08 \times 10^{13}$$

whereupon

$$A_1 = 21{,}700 \text{ cal/mol}$$

$$B_1 = 1.08 \times 10^{13}$$

For purposes of the calculation B_2 and B_3 were set equal to zero. Data on the heat of explosion, density, and specific heat of TNT were obtained from Cook.[4] Values of the other input parameters were approximations obtained as discussed in previous reports.

Comparison of the fade point with the curve of wave pressure shows that fading occurs at a pressure of $\sim$90 kbars. This value is somewhat uncertain because of the rather wide fluctuations which occur in the computed maximum pressure. Accuracy could be increased to any desired value by increasing the stability conditions imposed on the integration and decreasing the mesh size. This would, however, increase the running time, and was not deemed to be of importance to the present calculations. The experimental value reported by NOL is about 30 kbar.

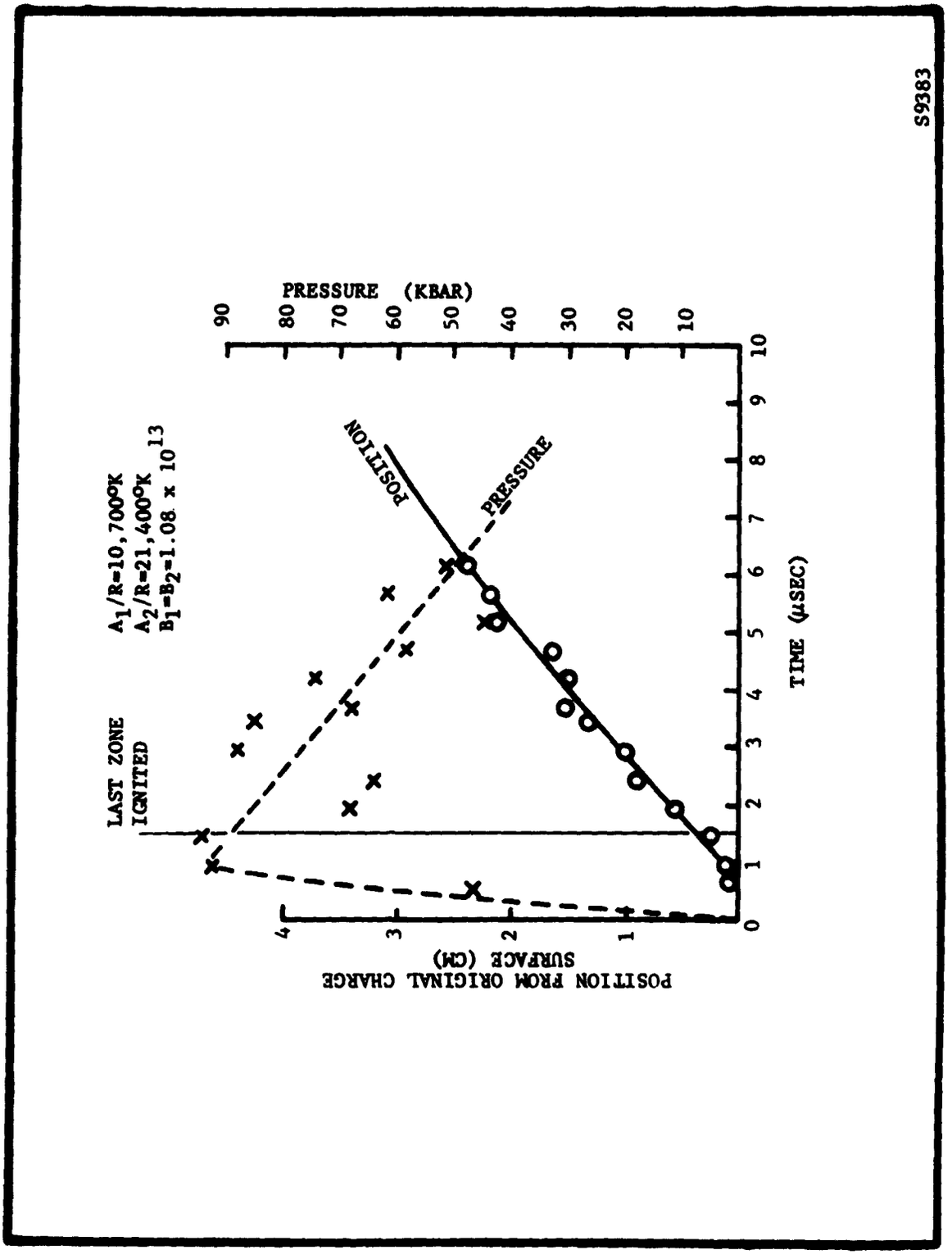

FIGURE 1. POSITION AND MAGNITUDE OF PEAK PRESSURE IN FADING WAVE IN TNT ($A_1/R = 10,700^oK$ - $A_2/R = 21,400^oK$)

It is deduced that either the rate parameters obtained from thermal decomposition data predict reaction rates much lower than are actually obtained in a detonation process, or that the assumed equation of state parameters lead to a value of energy density behind the lead shock much lower than that actually obtained. At the present time it is not possible to choose between these two explanation.

If the value taken for A_1 is 9500, then the results are as shown in Figure 2. The minimum shock pressure for initiation here agrees very well with the experimental value. The A_1 corresponds to an A_2 for TNT of $\sim$ 20 kcal which is not regarded as unreasonable.

Figures 3, 4 and 5 show additional results, using these values of A_1 and A_2. Figure 3 shows the reaction profile through the wave at a time of 12 μsec after initiation when the wave has propagated about 5 cm into the charge. Complete reaction behind the wave is not being achieved at this point, and therefore it would not be expected that the steady state velocity would have been reached. This is shown by a plot of wave trajectory in Figure 4, which indicates a velocity of about 4 mm/μsec. It is expected that upon further propagation, the wave velocity would increase and the reaction zone length would decrease. However, since the overall length was set at 10 cm, it was regarded as unlikely that growth to steady state would occur before reaching the end of the charge. This wave will be examined further by rerunning the problem with a longer charge length.

Figure 5 shows plots of v_g, v_s and e_s through the wave. The reduced amount of scatter shown in the points is a consequence of the imposition of increased stability criteria on the integration. These results together with those discussed above indicate that the mathematical procedures now being used are quite well behaved.

Calculation has also been carried out on the propagation of a detonation wave through a representative composite double-base propellant using the input data indicated in Table I, obtained from information provided by the Hercules Powder Company. In this problem, two grain burning reactions were used, one for the ammonium perchlorate oxidizer, and another for the double-base binder. As in the case of TNT, the rate parameters for the binder were obtained from thermal decomposition and adiabatic self-heating data. Those for ammonium perchlorate were obtained from data published by the Aerojet General Corporation on the regression rates of APC surfaces in their hot plate experiments, which have been discussed in a previous progress report.[1] The aluminum was treated as inert. Grain size taken for the ammonium perchlorate was the average size of the

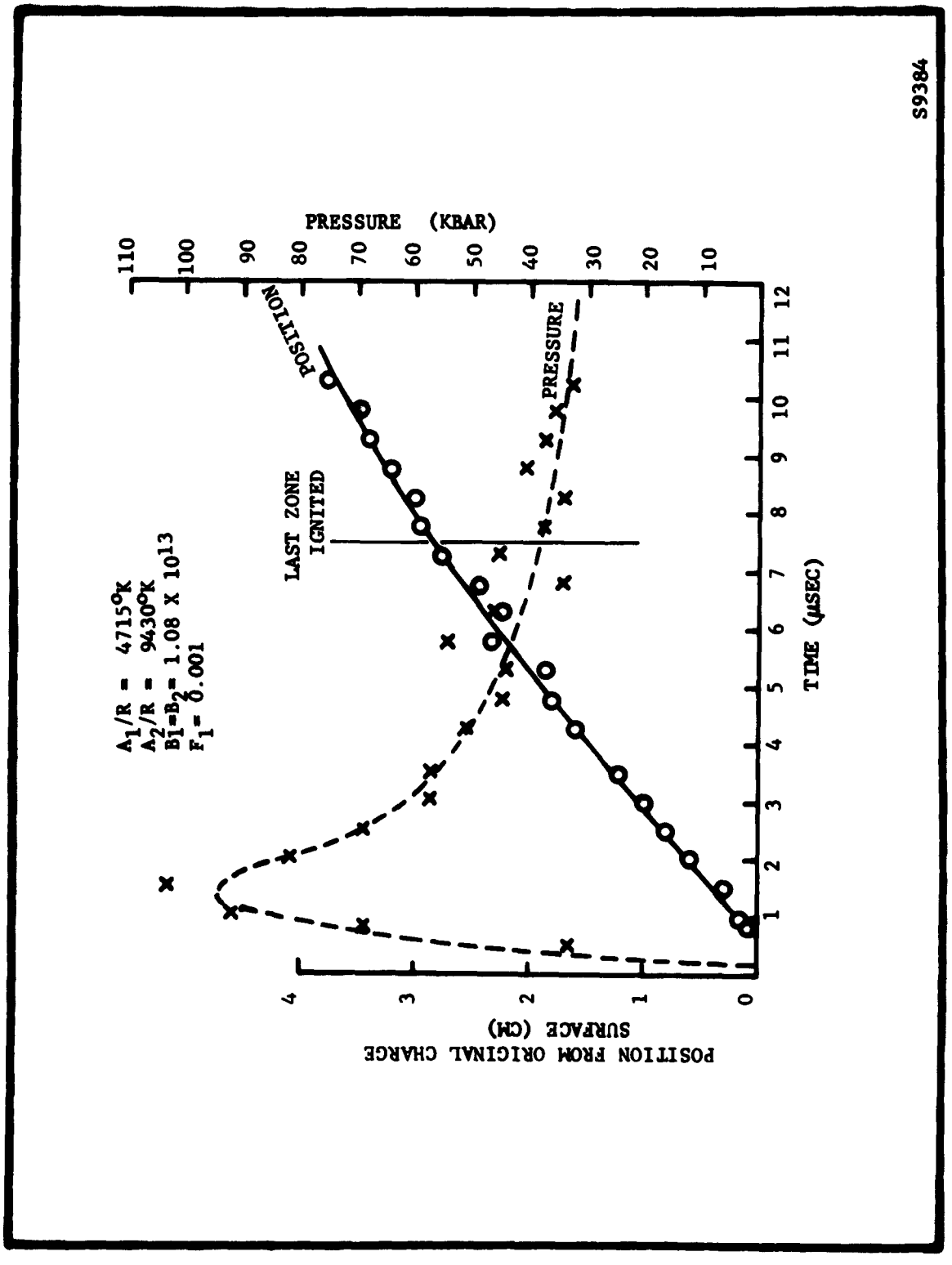

FIGURE 2. POSITION AND MAGNITUDE OF PEAK PRESSURE IN FADING WAVE IN TNT (A_1/R = 4715°K - A_2/R = 9430° K)

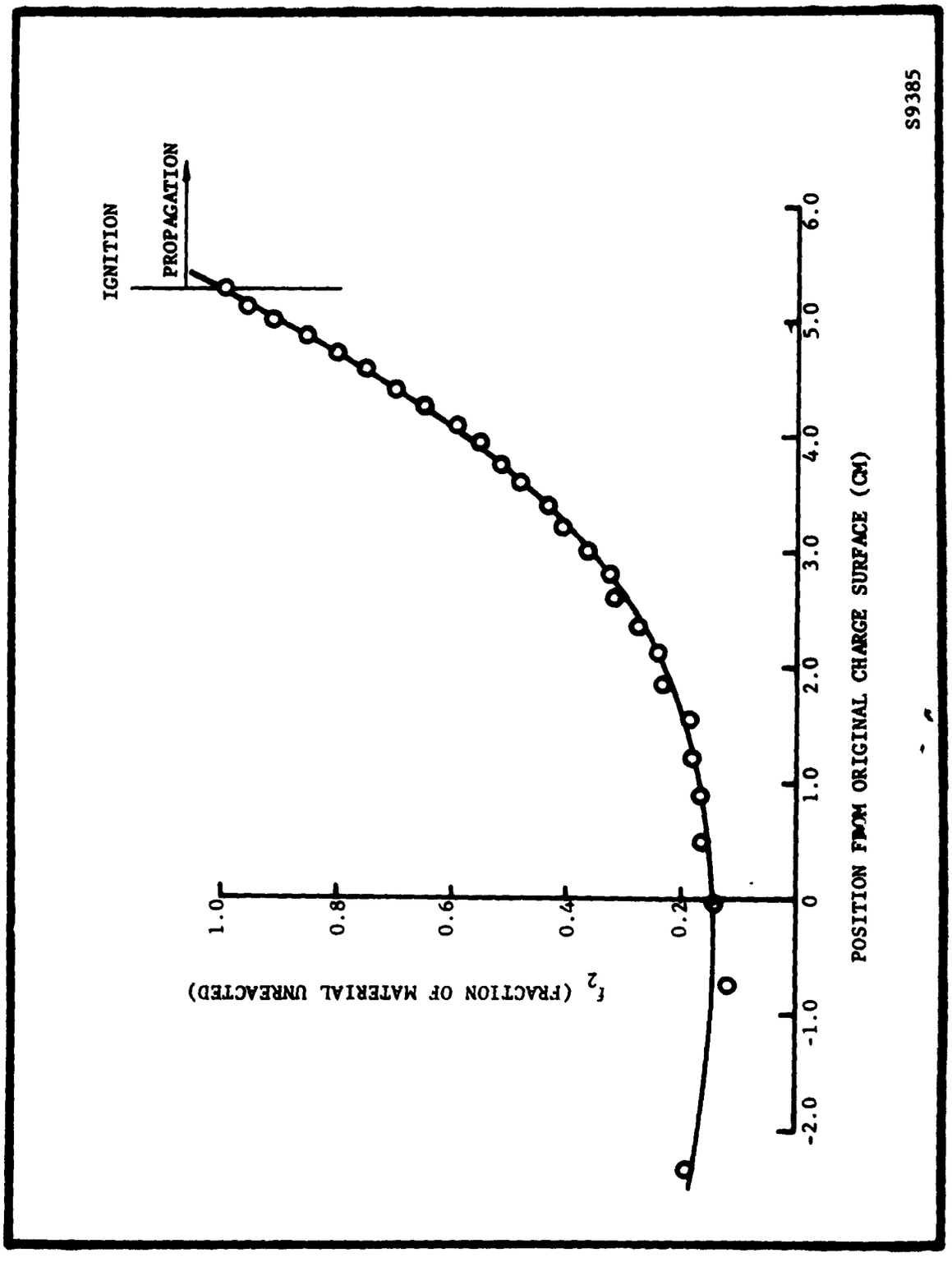

FIGURE 3. REACTION ZONE PROFILE THROUGH DETONATION WAVE IN TNT

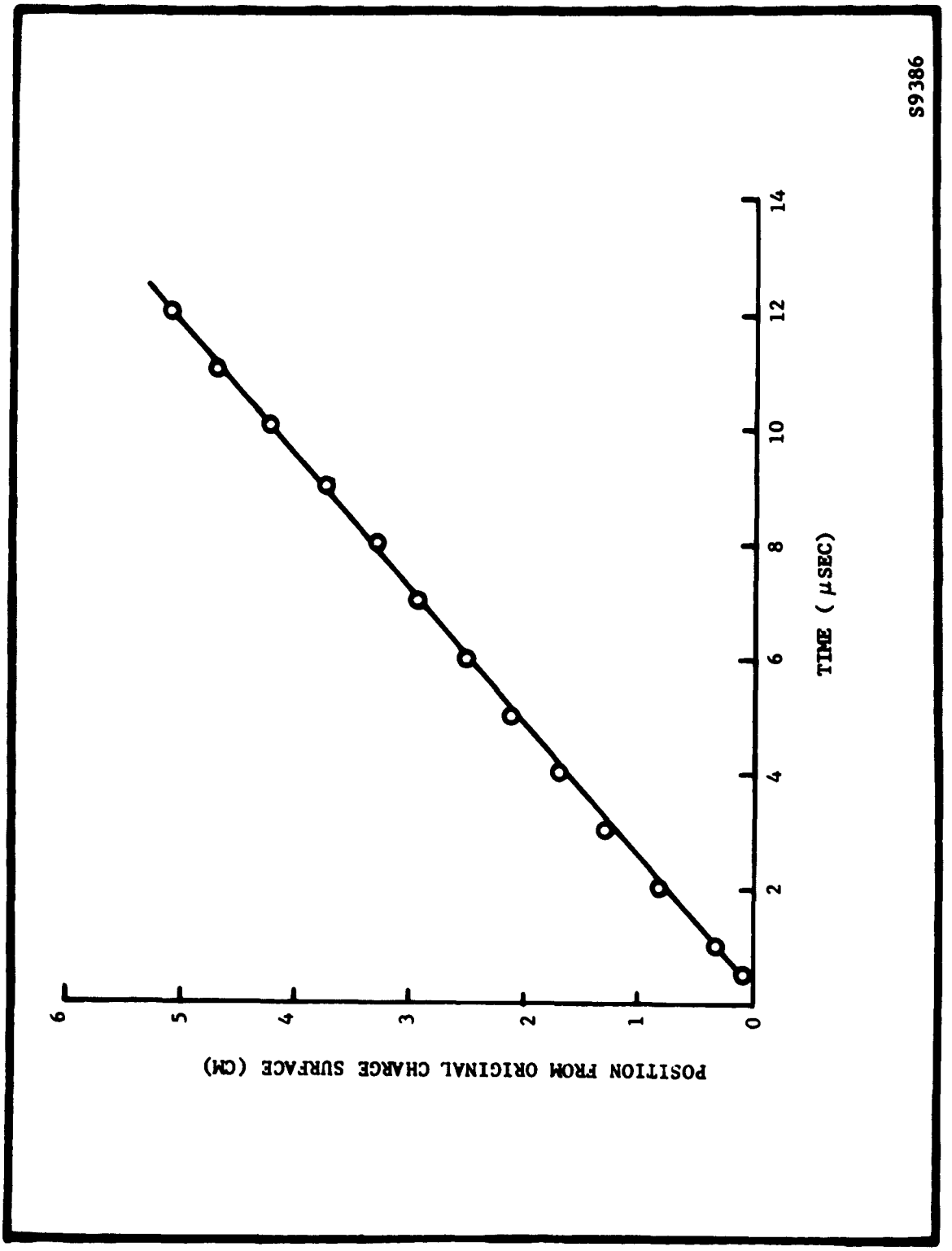

FIGURE 4. INITIAL TRAJECTORY OF DETONATION WAVE IN TNT

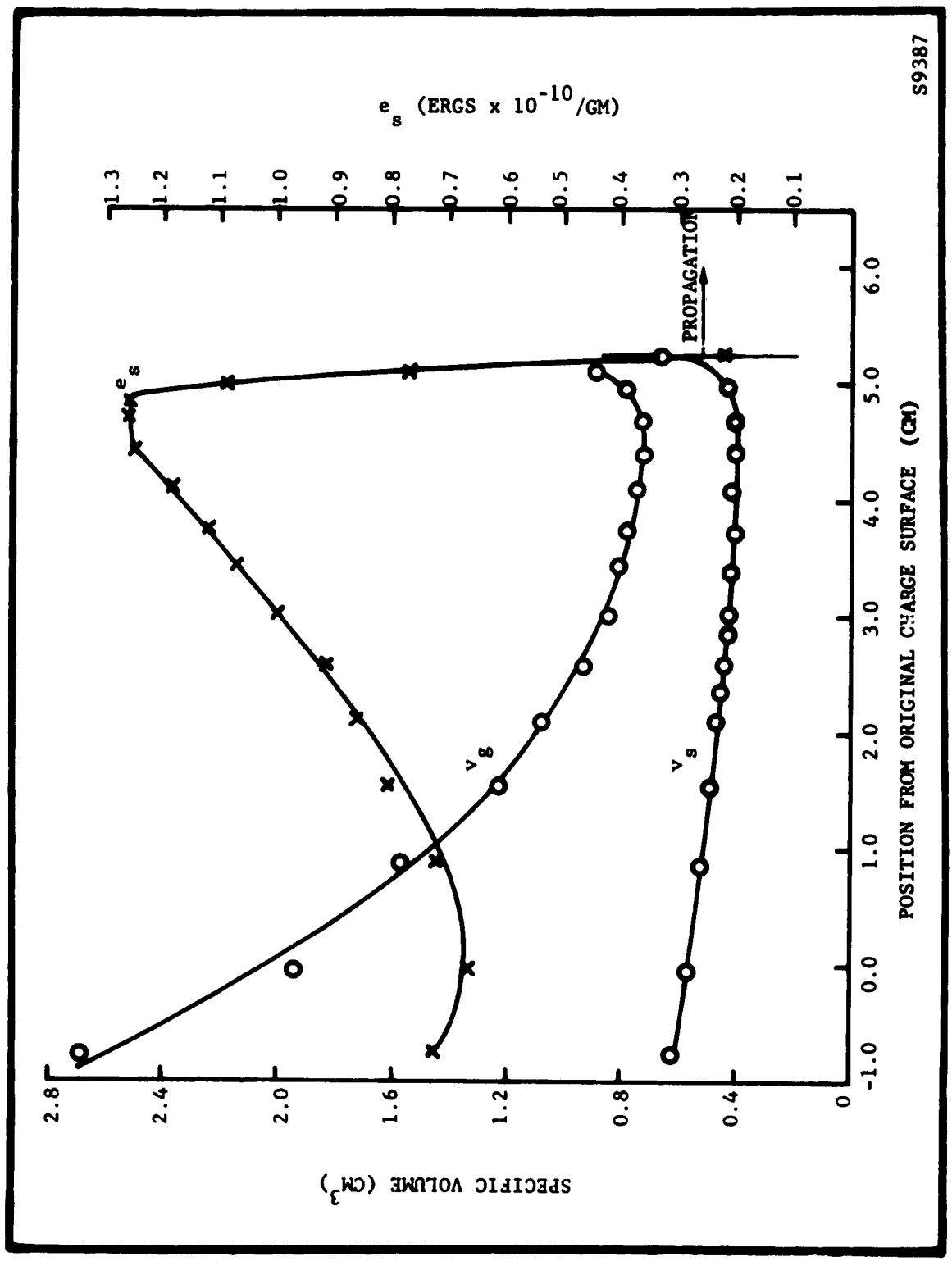

FIGURE 5. SOLID-PHASE ENERGY DENSITY AND SOLID AND GAS SPECIFIC VOLUMES THROUGH A DETONATION WAVE IN TNT

material used in the original mix; that for the binder was 1/2 the average distance between APC grains. The rate parameters for the ignition reaction were taken as those of the ammonium perchlorate for two reasons. First, under conditions of low shock intensity the APC rate law gives a faster reaction than that for the binder. This rate would therefore be most important in the ignition process. Second, NOL data from card gap experiments[6,7,8] support this conclusion. The heat of the ignition reaction was taken as the average of the heats of reaction of the APC and binder since they are assumed to contribute equally to the ignition reaction.

Figure 6 shows the trajectory and peak pressure in a computed wave initiated with a 100 kbar shock. Initial wave velocity is found to be about 5 mm/μsec slowing to about 4 mm/μsec after 10 μsec. Peak pressures decay rapidly from the initial imposed value of 100 kbar to about 50 kbar. It is again pointed out that the scatter shown in the computed points is an inherent consequence of numerical integration methods, which, for these problems, is particularly severe in the region of peak pressure. It could be reduced, as desired, by tightening the stability criteria for the integration; however, at an increase cost in computing time.

Figure 6 indicates that this wave approached a steady-state condition. However, at the point at which the calculations were terminated, the pressure and velocity still seemed to be decreasing slightly, and it is possible that fading would ultimately have occurred. The conclusion is that the material is marginal for detonability. It is of considerable interest here that experimental data on similar propellant materials obtained at the Naval Ordnance Laboratory are consistent with the conclusions to be drawn from these calculations that a pressure of 50 kbar is somewhat above the maximum pressure required for initiation.[6,7,8] It would be premature to speculate as to the significance of this agreement at the present time. However, an important difference between these results and those discussed previously for TNT lies in the fact that the rate data used for the ignition reaction in the present case were obtained by the hot plate technique, while those for TNT were derived from thermal decomposition data. Further study of this point appears desirable because it may shed some light on the question of which experimental methods are most suited for obtaining kinetic information appropriate for predicting detonation behavior.

Figure 7 shows some data on reaction and pressure profiles through the detonation wave in the above composite double-base propellant. It is of interest here that in the surface layers, the binder has burned completely and the APC only to a slight extent. In the interior of the charge, neither binder of APC has reacted significantly.

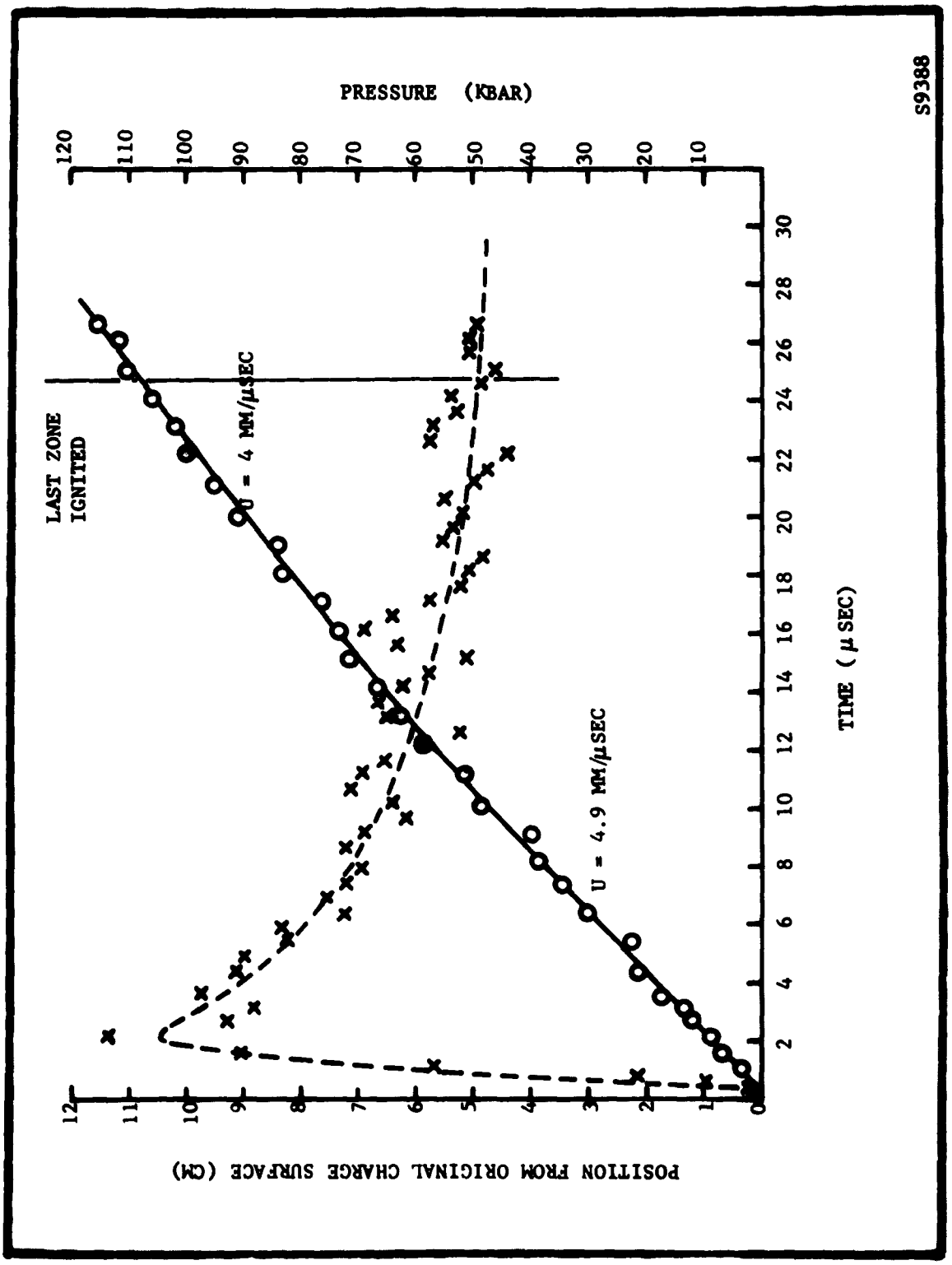

FIGURE 6. TRAJECTORY AND PEAK PRESSURES OF DETONATION WAVE IN COMPOSITE DOUBLE-BASE PROPELLANT

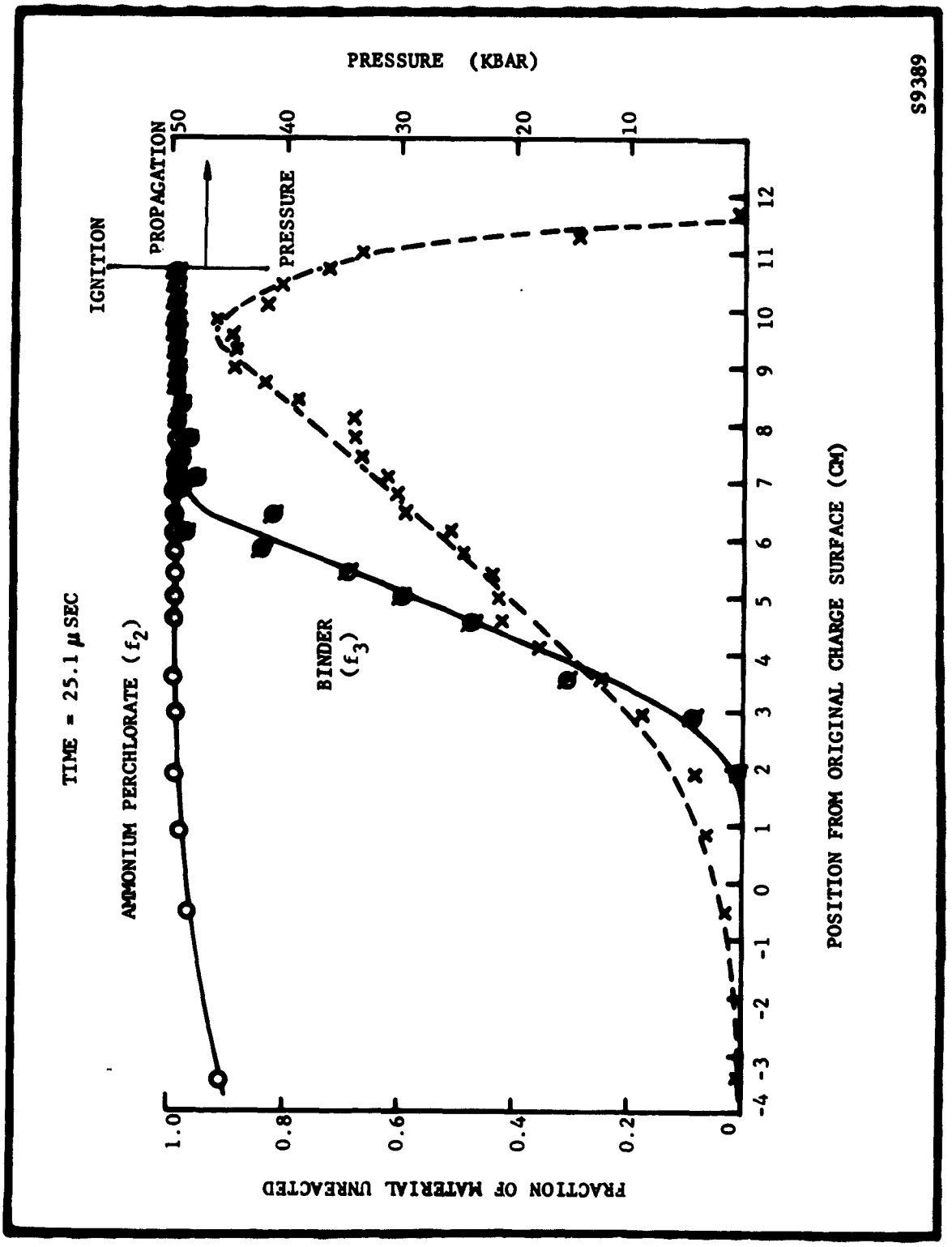

FIGURE 7. REACTION PROFILES FOR BINDER AND OXIDIZER AND PRESSURE PROFILE THROUGH A DETONATION WAVE IN COMPOSITE DOUBLE-BASE PROPELLANT

The explanation for this behavior appears to reside in the high activation energy, (A_2), and thus the high temperature coefficient for the binder reaction. Reaction in the surface is rapid because of the high energy deposited in the material by the initial shock. However, the energy released by binder reaction is not sufficient to drive a shock of this intensity so that following release of the surface pressure the wave decays. As a consequence of the decreasing pressure in the wave, the energy in the solid drops to a value at which the binder no longer reacts at a significant rate. Similar behavior is not observed on the part of the ammonium perchlorate reaction because its lower activation energy makes it less sensitive to changes in solid energy density. Following the point at which the grain burning reactions subside, the wave is supported only by the ignition reaction, and this constitutes the observed steady state process.

SECTION 4

EQUATION OF STATE STUDIES

The equation of state presently used for the solid phase is similar in form to that derivable by representation of the solid as a collection of harmonic oscillators. If the possible frequencies are ν_g, the equation obtained from such a model is the following:[9]

$$\left[p + \frac{\partial \phi}{\partial v}\right] v = \sum \gamma_g \frac{\frac{h \nu_g}{}}{\frac{h \nu_g}{e^{RT}} - 1} \tag{29}$$

where

$$\gamma_g = -\left(\frac{\partial \ln \nu_g}{\partial \ln v}\right)_T \tag{30}$$

Here the summed terms represent the internal thermal energy of the material and ϕ is a potential function such that the internal potential energy is given by

$$e_\phi = \int_\infty^v \frac{\partial \phi}{\partial v} \, dv \tag{31}$$

For present purposes, internal thermal energy is meant to include the kinetic and potential energy associated with atomic and molecular vibration; and internal potential energy represents that energy due to atomic and molecular distortion.

At high temperature the summation in equation (29) reduces to

$$RT \sum_g \gamma_g - \xi \tag{32}$$

where ξ is the zero point energy. If all of the γ_g are equal, substitution of (32) in (29) gives:

$$\left[p + \frac{\partial \phi}{\partial v}\right] v = \gamma_G \left[3NkT - \xi\right] \tag{33}$$

The oscillator model upon which equation (33) is based is closely approximated only by a perfect single crystal. However, the form of the equation is a consequence of the condition that the potential and thermal forms of internal energy are respectively dependent upon the volume only and upon the temperature only, and are therefore separable into different terms. If it is assumed that however poorly the simple oscillator model may represent reality in other respects, this separation of thermal and potential energy is valid for real materials, then the equation is of general application, provided only that the functions $\frac{\partial \phi}{\partial v}$ and γ_G, which now must be regarded as somewhat empirical in nature, are known.

In treating detonation behavior, it is more convenient to express the equation of state in terms of total energy, since the conservation equation refers to total energy. Adding equation (31) to both sides of (33), one has ultimately

$$\left[p + \frac{\partial \phi}{\partial v} + \frac{\gamma_G}{v} \int_{v_o}^{v} \frac{\partial \phi}{\partial v} dv\right] v = \gamma_G e + \gamma_G \left[3 N k T_o + \xi\right] \tag{34}$$

This is now the form of the solid equation of state presently in use where

$$\beta = \left[\frac{\partial \phi}{\partial v} + \frac{\gamma_G}{v} \int_{v_o}^{v} \frac{\partial \phi}{\partial v} dv\right] \tag{35}$$

$$\gamma_G = \gamma - 1$$

$$C = \gamma_G \left[3NkT_o + \xi\right]$$

$3NkT_o$ is the thermal energy content at ambient temperature.

e = total internal energy referred to zero at ambient conditions.

An objective of the present program is to determine the functions β and γ_G for the materials and the condition of significance to detonation phenomena. These can be obtained from p-v-T data. Partial differentiation of equation (33) gives:

$$\gamma_G = \frac{v}{3Nk}\left(\frac{\partial P}{\partial T}\right)_v \tag{36}$$

or

$$\gamma_G = \frac{v}{C_v}\left(\frac{\partial P}{\partial T}\right)_v \tag{37}$$

Thus γ_G at any v is given by the slope of the p-T curve. Substitution in (33) then provides $\frac{\partial \phi}{\partial v}$.

The necessary p-v-T data will be obtained by static pressure methods, making use of a piston-cylinder device designed by Kennedy[10] capable of an ultimate pressure in the order of 80 kilobars. This apparatus has been delivered and is in the process of being set up and checked out. Some preliminary development of methods and techniques will be necessary. It is estimated that initial equation of state data will be available near the end of the next report period.

NOMENCLATURE

t = time
p = pressure
q = von Neumann "q"
v = volume
u = material velocity
e = specific energy
h = Planck's constant
k = Boltzman constant
τ = ignition delay
w = empirical pressure constant
β = equation of state constant
C = equation of state constant
γ = equation of state constant
T = temperature
R = gas constant
ν = vibration frequency
ϕ = potential function
f = fraction of material unreacted
F = fraction of material in zone
A = activation energy
B = pre-exponential constant
m = reaction order
Q = heat of reaction
E = chemical energy released
ξ = zero point energy
C_v = specific heat
L = charge length
Z = grain radius
ρ = density
a = molecular diameter
P = applied pressure
U = wave velocity

Subscripts

o	ambient condition
1	ignition process
2	oxidizer process
3	binder process
4	diffusion process
g	gas phase
s	solid reaction phase
i	enert phase
G	Grüneisen constant
a	initial conditions
z	final conditions

Superscripts

n	time mesh number
j	space mesh number
o	ignition point
bar	average value

REFERENCES

1. Study of Detonation Behavior of Solid Propellants - Fourteenth Quarterly Report, Aeronutronic No. U-1229, 20 April 1961.

2. Study of Detonation Behavior of Solid Propellants - Sixteenth Quarterly Report, Aeronutronic No. 1464, 30 November 1961.

3. Melvin A. Cook, G. Smoot Horsley, W. S. Partridge and W. O. Ursenbach, "Velocity-Diameter and Wave Shape Measurements and the Determination of Reaction Rates in TNT", J. Chem. Phys., 24, p. 60 (1956).

4. M. A. Cook, "The Science of High Explosives", Chap. 6, Reinhold (1958).

5. I. Jaffee, R. Beauregard and A. Amster, "Determination of the Shock Pressure Required to Initiate Detonation of the Acceptor in the Shock Sensitivity Test", ARS Journal, 32, 22 (1962).

6. Informal Technical Progress Report on Task NOL-323, of 2 December 1959. Naval Ordnance Laboratory, White Oak, Maryland.

7. Informal Technical Progress Report on Task NOL-323, of 2 February 1962. Naval Ordnance Laboratory, White Oak, Maryland.

8. Informal Technical Progress Report on Task NOL-323, of 22 December 1961. Naval Ordnance Laboratory, White Oak, Maryland.

9. J. C. Slater, "Introduction to Chemical Physics", Chap. XIII, Mc-Graw-Hill (1939).

10. George C. Kennedy and Philip N. LaMori, "The Pressure of Some Solid-Solid Transitions", Publication No. 222, Institute of Geophysics and Planetary Physics, University of California, Los Angeles.

JANAF/SPIA DISTRIBUTION LIST

April 1962

Director
Advanced Research Projects Agency
The Pentagon, Room 3D159
Washington 25, D. C.

Attn: Advanced Propellant Chemistry Office — D-1, 4 Copies

U. S. Dept of the Interior
Bureau of Mines
4800 Forbes Street
Pittsburgh 13, Pennsylvania

Attn: M. M. Dolinar, Rpts Librarian
Explosives Research Lab — D-2, 1 Copy

National Aeronautics and Space Administration
Washington 25, D. C.

Attn: Office of Tech Info and Educational Programs
Code ETL — D-3, 7 Copies

Headquarters
6593rd Test Group (Dev)
Air Force Systems Command
United States Air Force
Edwards Air Force Base
California

Attn: (DGS) — AF-4, 1 Copy

Headquarters, Space Systems Division
Air Force Systems Command
P. O. Box 262
Air Force Unit Post Office
Los Angeles 45, California

Attn: TDC — AF-11, 1 Copy

Commander
Armed Services Tech Information Agency
Arlington Hall Station
Arlington 12, Virginia

Attn: TIPCR — AF-12, 10 Copies

6593rd Test Group (Dev)
Air Force Systems Command
Edwards Air Force Base
California

Attn: DGPS — AF-14, 1 Copy

Commander
Aeronautical Systems Division
Wright-Patterson Air Force Base
Ohio

Attn: ASRCEM-1 — AF-15, 1 Copy

JANAF/SPIA DISTRIBUTION LIST (Continued)

Commanding General
Aberdeen Proving Ground
Maryland

Attn: Ballistic Research Lab
ORDBG-BLI — A-1, 1 Copy

Commander
U. S. Army Ordnance Missile Command
Redstone Arsenal
Alabama

Attn: Technical Library — A-11, 5 Copies

Bureau of Naval Weapons
Department of the Navy
Washington 25, D. C.

Attn: DLI-3 — N-2, 2 Copies

Bureau of Naval Weapons
Department of the Navy
Washington 25, D. C.

Attn: RMMP-2 — N-3, 2 Copies

Bureau of Naval Weapons
Department of the Navy
Washington 25, D. C.

Attn: RMMP-331 — N-4, 1 Copy

Commanding Officer
U. S. Naval Propellant Plant
Indian Head, Maryland

Attn: Technical Library — N-7, 2 Copies

Commander
U. S. Naval Ordnance Laboratory
White Oak
Silver Spring, Maryland

Attn: Library — N-9, 1 Copy

Commander
U. S. Naval Ordnance Test Station
China Lake, California

Attn: Tech Library
Branch — N-10, 1 Copy

Department of the Navy
Office of Naval Research
Washington 25, D. C.

Attn: Code 429 — N-12, 1 Copy

Director
Special Projects Office
Department of the Navy
Washington 25, D. C.

N-18, 1 Copy

JANAF/SPIA DISTRIBUTION LIST (Continued)

U. S. Naval Ordnance Laboratory
Corona
California

Attn: P. J. Slota, Jr — N-22, 1 Copy

Bureau of Naval Weapons
Department of the Navy
Washington 25, D. C.

Attn: RRRE-6 — N-23, 1 Copy

Aerojet-General Corp
P. O. Box 296
Azusa, California

Attn: Librarian — C-1, 3 Copies

Hercules Powder Company
Allegany Ballistics Laboratory
P. O. Box 210
Cumberland, Maryland

Attn: Library — C-2, 3 Copies

Atlantic Research Corp
Shirley Highway and Edsall Road
Alexandria, Virginia

C-5, 1 Copy

Jet Propulsion Laboratory
4800 Oak Grove Drive
Pasadena 3, California

Attn: I. E. Newlan, Chief Reports Group — C-20, 1 Copy

Rohm and Haas Company
Redstone Arsenal Research Division
Huntsville, Alabama

Attn: Librarian — C-36, 2 Copies

Solid Propellant Information Agency
Applied Physics Laboratory
The Johns Hopkins University
Silver Spring, Maryland

C-37, 3 Copies

Solid Propellant Information Agency
Applied Physics Laboratory
The Johns Hopkins University
Silver Spring, Maryland

Attn: Technical Rpts Group — C-37, 2 Copies

Thiokol Chemical Corporation
Redstone Division
Huntsville, Alabama

Attn: Technical Director — C-39, 2 Copies

JANAF/SPIA DISTRIBUTION LIST (Continued)

Thiokol Chemical Corporation
Elkton Division
Elkton, Maryland

Attn: Librarian — C-41, 1 Copy

Olin Mathieson Chemical Corporation
Marion, Illinois

Attn: Research Library, Box 508 — C-43, 1 Copy

Reaction Motors Division
Thiokol Chemical Corporation
Denville, New Jersey

Attn: Librarian — C-44, 1 Copy

Rocketdyne, A Division of
North American Aviation Inc.
Solid Propulsion Operations
P. O. Box 548
McGregor, Texas

Attn: Library — C-49, 1 Copy

Department of Chemical Engineering
New York University
New York 53, New York

Attn: C. J. Marsel — C-57, 1 Copy

Rocketdyne
6633 Canoga Avenue
Canoga Park, California

Attn: Library, Dept 596-306 — C-61, 3 Copies

Lockheed Propulsion Company
P. O. Box 111
Redlands, California

Attn: Miss Belle Berlad, Librarian — C-65, 1 Copy

Aerojet-General Corporation
P. O. Box 1947
Sacramento, California

Attn: Tech Info Office — C-72, 3 Copies

Thiokol Chemical Corporation
Wasatch Division
P. O. Box 524
Brigham City, Utah

Attn: Library Section — C-73, 2 Copies

Olin Mathieson Chemical Corporation
Research Library 1-K-3
275 Winchester Avenue
New Haven, Connecticut

Attn: Mail Control Room, Miss Laura M. Kajuti — C-76, 3 Copies

JANAF/SPIA DISTRIBUTION LIST (Continued)

Wright Aeronautical Division
Curtiss-Wright Corporation
Wood-Ridge, New Jersey — C-78, 2 Copies

Ethyl Corporation
Research Laboratories
1600 West Eight Mile Road
Ferndale, Michigan

Attn: E. B. Rifkin, Asst Dir
Chemical Research — C-90, 1 Copy

The Dow Chemical Company
Security Section
Box 31
Midland, Michigan

Attn: Dr. R. S. Karpiuk
1710 Building — C-91, 1 Copy

Minnesota Mining and Manufacturing Co
900 Bush Avenue
St. Paul 6, Minnesota

Attn: Dr. William S. Friedlander — C-94, 2 Copies

VIA: Mr. H. C. Zeman
Security Administrator

American Cyanamid Company
1937 W. Main Street
Stamford, Connecticut

Attn: Dr. A. L. Peiker — C-96, 1 Copy

Hercules Powder Company
Bacchus Works
Magna, Utah

Attn: Librarian — C-98, 1 Copy

Allied Chemical Corporation
General Chemical Division
Research Laboratory
P. O. Box 405
Morristown, New Jersey

Attn: L. J. Wiltrakis
Security Office — C-106, 1 Copy

General Electric Company
Cincinnati 15, Ohio

Attn: Tech Info Center — C-107, 1 Copy

Callery Chemical Company
Research and Development
Callery, Pennsylvania

Attn: Document Control — C-112, 1 Copy

Pennsalt Chemicals Corporation
Box 4388
Philadelphia 18, Pennsylvania

Attn: Dr. G. Barth-Wehrenalp — C-114, 1 Copy

JANAF/SPIA DISTRIBUTION LIST (Continued)

Space Technology Laboratory, Inc.
5730 Arbor-Vitae Street
Los Angeles 45, California

Attn: Mr. Robert C. Anderson — C-116, 1 Copy

Union Carbide Corporation
270 Park Avenue
New York 17, New York

Attn: B. J. Miller — C-121, 1 Copy

United Technology Corporation
P. O. Box 358
Sunnyvale, California

Attn: Librarian — C-124, 1 Copy

Aerospace Corporation
P. O. Box 95085
Los Angeles 45, California

Attn: Library - Documents — C-129, 2 Copies

Thiokol Chemical Corporation
Rocket Operations Center
P. O. Box 1640
Ogden, Utah

Attn: Librarian — C-133, 1 Copy

Institute for Defense Analyses
Research and Engineering
Support Division
1825 Connecticut Ave, N.W.
Washington 9, D. C.

Attn: Technical Information Office — C-134, 1 Copy

Rocket Power/Talco
Research Laboratories
3016 East Foothill Boulevard
Pasadena, California

Attn: Dr. Milton Farber — C-126, 1 Copy

British Defense Staff
British Embassy
3100 Massachusetts Avenue
Washington, D. C.

Attn: Scientific Information Officer — F-1, 4 Copies

VIA: Chief, Bureau of Naval Weapons
Department of the Navy
Washington 25, D. C.

Attn: DSC-3

JANAF/SPIA DISTRIBUTION LIST (Continued)

Defense Research Member
Canadian Joint Staff (W)
2450 Massachusetts Avenue, N. W.
Washington 8, D. C.

F-2
4 Copies

VIA: Chief, Bureau of Naval Weapons
Department of the Navy
Washington 25, D. C.

Attn: DSC-3

J. I. Thompson and Company
1118 22nd Street, N.W.
Washington 25, D. C.

Attn: Mr. K. Dahl-Hansen 1 Copy

VIA: U. S. Bureau of Naval Weapons
Resident Representative
Applied Physics Laboratory
Silver Spring, Maryland